Research Article

THERMAL FORCE EFFECTS ON SATELLITES

J. Duha[1] & G. B. Afonso[2]

Thermal force effects due to the Earth infrared radiation acting on artificial satellites can explain most of the residual orbit decay observed on high altitude satellites. In this work, we propose an improved thermal model that presents the total thermal effect as a sum of the summer-winter and the "generalized" day-night effects. We show that a unified model may take into account the sin θ' term (where θ' is the co-latitude of the thermal energy source) for the day-night force component and the cos θ' term for the summer-winter force component. These terms are associated with temperature variations on the satellite's surface due to its movement around the thermal energy source and allow the simultaneous application of these two forces resulting in a unified total thermal force that has two components: the Summer-Winter force, in the satellite spin axis direction (z), and the generalized Day-Night force, in the satellite equatorial plane (xy). We calculate the along-track accelerations for a test-satellite (parameters based on the LAGEOS satellite data) and obtain the average along-track acceleration $\langle S \rangle = -3.46 \times 10^{-13}$ ms^{-2}, for the day-night effect, and $\langle S \rangle = -2.85 \times 10^{-12}$ ms^{-2}, for the summer-winter effect, that leads to a residual orbit decay of nearly 1.08 mmd^{-1}. Finally, we analyze the behavior of the average radial and along-track accelerations, and the thermal lag angle, as a function of the satellite's altitude, and show that there is a "selective law" that associates the maximum thermal effect to the radius and altitude of the satellite, and control the satellite orbit decay.

Key words: Thermal re-emission; Summer-winter effect; Day-night effect; Unified thermal model; Artificial satellites; Orbit decay.

EFEITOS DE ENERGIA TÉRMICA EM SATÉLITES-*Os efeitos de re-emissão térmica associados à radiação IR da Terra atuante em satélites artificiais, explicam grande parte do decaimento orbital residual observado em satélites de alta altitude. Neste trabalho, propõe-se um modelo térmico otimizado que apresenta o efeito térmico total como a soma dos efeitos Inverno-Verão e Noite-Dia "generalizado". Além disso, este trabalho procura mostrar que um modelo unificado deve levar em consideração o termo sen θ' (onde θ' é a colatitude da fonte de energia térmica) para a componente noite-dia da força térmica e o termo cos θ' para a componente inverno-verão da força térmica. Estes termos estão associados à variações de temperatura na superfície do satélite devidas ao seu movimento ao redor da fonte de energia térmica e permitem a aplicação simultânea dessas duas forças, resultando em uma força térmica total unificada que possue duas componentes: a força Inverno-Verão, na direção do eixo de spin do satélite (z), e a força Noite-Dia generalizada, no plano equatorial do satélite (xy). Neste trabalho, as forças de re-emissão térmica são aplicadas à um satélite-teste (parâmetros baseados em dados do satélite LAGEOS) de forma a se obter a perturbação resultante em termos da aceleração transversal média, para o efeito noite-dia, $\langle S \rangle = -3{,}46 \times 10^{-13}$ ms^{-2}, e para o efeito inverno-verão, $\langle S \rangle = -2{,}85 \times 10^{-12}$ ms^{-2}, que leva à um decaimento orbital residual de aproximadamente 1.08 mmd^{-1}. Finalmente, são analisados o comportamento das acelerações radial e transversal médias, e do ângulo de atraso, como uma função da altitude do satélite, e é obtida uma "lei de seleção" que associa o efeito térmico máximo ao raio e a altitude do satélite.*

Palavras-chave: *Re-emissão térmica; Efeito inverno-verão; Efeito noite-dia; Modelo térmico unificado; Satélites artificiais; Decaimento orbital.*

[1]Dep. de Geomática, Centro Politécnico, UFPR
Cx. Postal 19011,Cep: 81.531-990, Curitiba, Brasil
jduha@geoc.ufpr.br
[2]Dep. de Física, UFPR, Curitiba, Brasil

INTRODUCTION

All objects in the space are regularly heated up by thermal radiation sources. Spacecrafts are not excluded. The investigation of the thermal effects, in this case, can explain some unexpected features of the orbital evolution of spacecrafts travelling across the space. We can also obtain, a better orbital modeling of the artificial satellites moving about the Earth.

The mechanism that generates the thermal force that acts on the satellites is very simple: The incoming radiation from a thermal radiation source (Sun, Earth, etc.) heats up more efficiently the satellite's surface in the side facing the radiation source, than in the opposite side (dark side). As a consequence, the satellite surface presents an asymmetric temperature distribution. The hotter side re-emits photons more energetic and thus, loses more momentum than the cooler one. This anisotropy leads to a net amount of linear momentum that causes a net recoil force to act on the satellite. The amount of radiation received by a surface element per unit time varies accordingly to the energy source coordinates, that are controlled by the satellite spin axis orientation, and rotational and orbital motion of the satellite. For a spinning satellite, in its reference frame, there are two main asymmetries on the satellite's surface temperature distribution: along the spin axis (known as summer-winter effect) and along the equatorial direction (day-night effect).

When the satellite LAGEOS was launched (May 4, 1976) an unexpected and non-modeled residual orbit decay became evident (Afonso et al., 1980; 1985). The day-night effect (Yarkovsky or diurnal effect) was taken into account, but due to the satellite rapid rotation, one could not explain the observed orbit decay residuals. In this case, the rotational period was less than the characteristic time of the satellite thermal inertia, thus the day-night thermal asymmetry was very small (Afonso et al.,1989).

However, the anisotropy associated with the satellite orbital motion leads to a force along the spin axis known as summer-winter force (seasonal effect). This effect does not depend on the satellite rotation and can explain almost all the observed residuals. Both day-night and summer-winter effects are consequence of the same physical mechanism: a photon "thrust" generated by the anisotropy associated with the re-emission of the radiant energy by the satellite's surface.

In order to predict the dynamics of satellites ruled by thermal re-emission forces, we introduce, in this work, a model that allows us to understand how the variations on the satellite spin axis orientation (Bertotti & Iess, 1991; Farinella et al., 1996) affect the thermal re-emission forces direction and absolute values; which relationship we can find between the day-night and summer-winter effects, and how this relationship can be mathematically expressed and physically understood. We are going to provide the modeling of the Summer-Winter force, $\mathbf{F}_z$, and also a "generalized" Day-Night force, $\mathbf{F}_{xy}$, valid for any spin axis inclination, and hence the unification of these two forces in only one: the Total Thermal force, **F** (Duha, 1996). We also show that there is a "selective law" associated with the radius of the satellite (maximum thermal effect) and the distance to the energy source (Duha, 1996).

We apply the total thermal force to a test-satellite and obtain the averaged along-track and radial accelerations due to the thermal re-emission effects. We discuss the relationship between the generalized day-night and summer-winter effects, and predict the residual orbit decay, due to thermal re-emission forces, for a test-satellite with parameters based on the LAGEOS satellite data.

THE UNIFIED THERMAL RE-EMISSION MODEL

In the thermal re-emission model, proposed here, we assume that the satellite is an homogeneous sphere, heated up by a punctual radiant energy source. The satellite is a gray body with surface temperature $T = T_0 + \Delta T$, where T_0 is the average temperature and ΔT is the temperature variation. Here, $I = I_0 + \Delta I$ represents the radiance that leads to a heating T, and I_0 is the constant radiance from the energy source, that gives the body temperature T_0. Let us suppose that ΔT and ΔI vary with time as e^{-ivt} where $i=\sqrt{-1}$, so that they can be written as:

$$\Delta T(R,\theta,\phi,t) = \Delta\hat{T}(R,\theta,\phi,t)e^{-ivt}, \qquad (1)$$

where R is the radial distance to a point at the surface measured from the center of the satellite, v is the frequency of the angular movement, θ is the co-latitude, and ϕ is the longitude of the surface point.

To obtain the temperature distribution at the surface of the sphere, we solve the heat conduction equation applying the appropriate boundary conditions. In the spherical coordinates we obtain (Rubincam,1987; Afonso & Foryta,1989; Duha, 1996):

$$\Delta\hat{T}(R,\theta,\phi) = \sum_{l=0}^{\infty}\sum_{m=-l}^{l} C_{l,m} P_l^m(\cos\theta)\, j_l(KR) e^{im\phi}, \qquad (2)$$

where P_l^m *(cos θ)* are the associated Legendre functions (of *l* th degree and *m* th order), $j_l(Kr)$ is the spherical Bessel function, and $C_{\{l,m\}}$ is given by the following expression:

$$C_{l,m} = \frac{\alpha I_0 f_{l,m}}{4\varepsilon\sigma T_0^3 j_l(KR) + k\left.\frac{\partial j_l(KR)}{\partial R}\right|_{R=R_s}}, \quad (3)$$

$$K = \left(\frac{i\nu\rho C_p}{k}\right)^{1/2}, \quad (4)$$

where $f_{l,m}$ are the coefficients of a Legendre polynomial expansion (Rubincam,1987; Afonso & Foryta,1989; Duha, 1996). In the equations above the following satellite parameters are used: *a*, the satellite's surface absorption of radiation; *ε*, the satellite's surface emission of radiation; C_p, the specific heat at constant pressure; *k*, the thermal conductivity; T_0, the average temperature due to the radiance at satellite altitude; *ρ*, the mass density; R_s, the satellite radius; and *σ* is the Stefan-Boltzmann constant.

By substituting Eq. (2) in Eq. (1) we obtain:

$$\Delta T(R_s,\theta,\phi,t) = \sum_{l=0}^{\infty}\sum_{m=-l}^{l} \frac{f_{l,m}\alpha I_0 P_l^m(\cos\theta)e^{im\phi}e^{-i\nu t}e^{i\delta}}{(4\varepsilon\sigma T_0^3 + kX)(1+\xi^2)^{\frac{1}{2}}} \quad (5)$$

where we introduced the following variables:

$$\xi = -\frac{kY}{4\varepsilon\sigma T_0^3 + kX} \quad (6)$$

$$\delta = \arctan\xi, \quad (7)$$

$$X + iY = \frac{1}{j_l(KR)}\left.\frac{\partial j_l(KR)}{\partial R}\right|_{R=R_s}, \quad (8)$$

with *X* and *Y* are the real and imaginary parts of the complex number *X+iY* given by Eq. (8). The angular variable *δ* defined in Eq. (7) represents the angle between the direction of the absorption and the re-emission of the radiation, that appears as a consequence of the satellite thermal inertia. From Eqs. (6) and (7) we have:

$$\delta_i = \arctan\left(-\frac{kY_i}{4\varepsilon\sigma T_0^3 + kX_i}\right). \quad (9)$$

Most of the unusual behavior of the thermal lag, thermal force and the semi-major axis variation associated with it, and so on, can be explained by the analysis of the quantities X_i and Y_i. If we expand Eq. (8) in series, we have:

$$X_i + iY_i = \frac{1}{R_s} + \sum_{n=1}^{\infty} a_n (K_i R_s)^{2n}. \quad (10)$$

The $1/R_s$ term will dominate the X_i behavior for small satellite radius and will lead to the significant decrease of the thermal lag, that we will show ahead.

THE TOTAL THERMAL RE-EMISSSION FORCE

The re-emission force can be obtained if we assume that the satellite re-emits the radiation according to Lambert's law. The photons leaving its surface carry away momentum proportionally to the surface temperature *T*. The resulting force over the total surface area (Rubincam,1987; Afonso & Foryta,1989; Duha, 1996) is:

$$\mathbf{F} = -\frac{2\varepsilon\sigma}{3c}\int_0^{\pi}\int_0^{2\pi} T^4\left(sin\theta\cos\phi\,\mathbf{i} + sin\theta\,sin\phi\,\mathbf{j} + \cos\theta\,\mathbf{k}\right)R^2 sin\theta\,d\theta\,d\phi \quad (11)$$

Thus the Total Thermal Re-emission force acting on the satellite (Duha,1996) is:

$$\mathbf{F} = n_f\{A_1\,sin(v_2t - \delta_2)[cos(v_1t - \delta_1)\mathbf{i} + sin(v_1t - \delta_1)\mathbf{j}] + A_2\,cos(v_2t - \delta_2)\mathbf{k}\}, \quad (12)$$

$$n_f = \frac{1}{2(1+sin^2 v_2 t)} \quad (13)$$

where n_f is the normalization factor, with maximum and minimum values 1/2 and 1/4, respectively. We take into account the two main angular satellite movements, rotation and translation, with angular frequencies, v_1 and v_2, respectively. The angle δ_1 is the thermal lag due to rotation; δ_2 is the thermal lag due to translation, and A_1, A_2 are given by:

$$A_i = \frac{-8\alpha I_0 R_s^2\pi}{9c\left(1 + \frac{kX_i}{4\varepsilon\sigma T_0^3}\right)\left(1+\xi_i^2\right)^{\frac{1}{2}}}. \quad (14)$$

The symbol *i* indicates that the quantities *X* and *ξ* are calculated with $\nu = \nu_1$ for the day-night effect and $\nu = \nu_2$ for the summer-winter effect. Note that the thermal re-emission force has two components, one in the satellite *xy* plane (equatorial) and the second in the *z* axis direction (spin). The *xy* force leads to the generalized day-night effect (we will refer to it only as day-night effect) and the *z* force to the summer-winter effect. This general expression shows that the summer-winter and day-night forces can be understood like

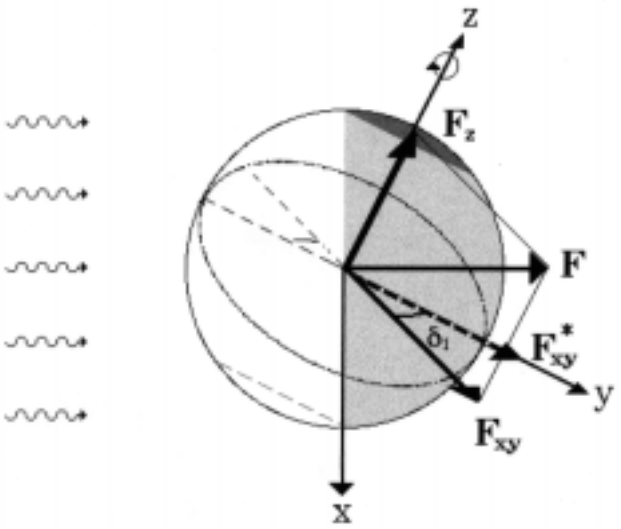

Figure 1 - The summer-winter ($\mathbf{F}_z$) and "generalized" day-night ($\mathbf{F}_{xy}$) forces representation in the (*x,y,z*) reference frame centered at a spherical body that rotates around the *z* axis.

Figura 1 *- Representação das forças inverno-verão ($\mathbf{F}_z$) e noite-dia ($\mathbf{F}_{xy}$) no sistema de referência (x,y,z) centrado em um corpo esférico que gira em torno do eixo z.*

the components $\mathbf{F}_{xy}$ and $\mathbf{F}_z$ of the *total* thermal re-emission force acting on the satellite.

Now, if we assume that the spin axis lies on the satellite orbital plane, we can re-write Eq. (12) as:

$$\mathbf{F} = n_f \{A_1 \sin(\theta' - \delta_2)[\cos(\phi' - \delta_1)\mathbf{i} + \sin(\phi' - \delta_1)\mathbf{j}] + A_2 \cos(\theta' - \delta_2)\mathbf{k}\}, \quad (15)$$

where the (θ',ϕ') coordinates represent the punctual radiant energy source apparent position in the satellite reference frame, where θ' is the co-latitude and ϕ' is the longitude.

The first term (***i,j***) in the right hand side of the equation is related to the day-night effect (diurnal effect) that has a maximum for $\theta' = \pi/2$ (thus, $\sin\theta' = 1$), and yields from an asymmetric temperature distribution along the *xy* plane; whereas the second term ***k*** is related to the summer-winter effect (seasonal effect), that has a maximum for $\theta' = 0$, (thus, $\cos\theta' = 1$), and yields from the asymmetric temperature distribution along the *z* axis.

Note that $\cos\theta'$ and $\sin\theta'$ increase or decrease the intensity of the summer-winter and day-night forces as the body moves along its trajectory. There is a direct relationship between the co-latitude of the energy source and the intensity of the summer-winter and day-night effects. When $\theta' = \pi/2$; or $3\pi/2$ we have $n_f = 1/4$ and the temperature distribution is more uniform than for $\theta' = 0$; or π because, in this case, $n_f = 1/2$; so the intensity of the thermal force must be smaller for $\theta' = \pi/2$, when the summer-winter effect vanishes ($\mathbf{F}_z = 0$), then for $\theta' = 0$ when we have the opposite situation, and day-night effect vanishes ($\mathbf{F}_{xy} = 0$).

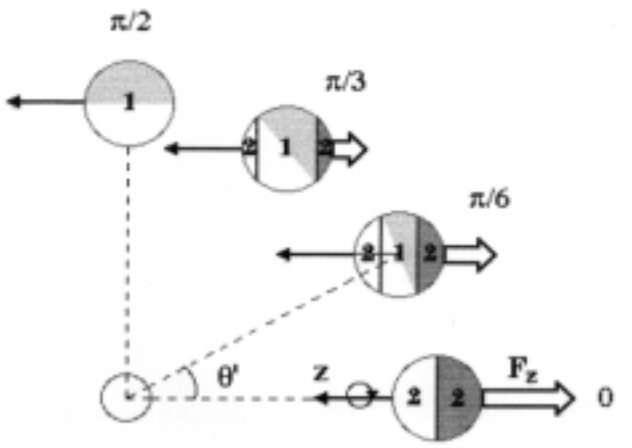

Figure 2 - As the satellite moves around the energy source, summer-winter and day-night effects loose and gain intensity alternatively. We can visualize this interplay between these two thermal effects if we associate the satellite's surface region (1) to the day-night effect and region (2) to the summer-winter effect. Note that, the area covered by (2) decreases as the energy source colatitude grows from 0 to $\pi/2$, while (1) increases. The opposite situation will take place if you consider the $\pi/2$ to π energy source colatitude values, and so on for the complete cycle.

Figura 2 *- A medida que o satélite se desloca ao redor da fonte de energia, os efeitos inverno-verão e noite-dia perdem e ganham intensidade alternadamente. Esta relação entre estes dois efeitos térmicos pode ser visualizada se associarmos a região (1) na superfície do satélite ao efeito noite-dia e região (2) ao efeito inverno-verão. Note que, a área coberta por (2) decresce à medida que a colatitude da fonte de energia cresce de 0 para $\pi/2$, enquanto que (1) decresce. Quando são considerados valores entre $\pi/2$ e π, para a colatitude da fonte de energia, tem-se a situação oposta, e assim por diante para o ciclo completo.*

Fig. 1 shows schematically a spherical body that rotates around the *z* axis, illuminated by a punctual radiant energy source. The thermal re-emission force, **F**, has two components $\mathbf{F}_{xy}$ and $\mathbf{F}_z$ associated with the day-night and summer-winter effects, respectively. Note that: $\mathbf{F} = \mathbf{F}^*_{xy} + \mathbf{F}_z$ for instantaneous thermal reaction (no thermal inertia, $\delta_1 = 0$).

Dividing Eq. (12) by the mass of the spherical satellite ($4\pi\rho R_s/3$) we get the satellite acceleration due to the total thermal force:

$$\mathbf{a} = n_f \{B_1 \sin(v_2 t - \delta_2)[\cos(v_1 t - \delta_1)\mathbf{i} + \sin(v_1 t - \delta_1)\mathbf{j}] + B_2 \cos(v_2 t - \delta_2)\mathbf{k}\}, \quad (16)$$

where:

$$B_i = \frac{-2\alpha I_0}{3 c \rho R_s \left(1 + \frac{kX_i}{4\varepsilon\sigma T_0^3}\right)(1 + \xi_i^2)^{\frac{1}{2}}} . \quad (17)$$

The $\mathbf{a}_{xy}$ component is associated with the day-night effect and the $\mathbf{a}_z$ with the summer-winter effect. Fig. 2 shows schematically a spherical satellite that rotates

around the *z* axis, on the orbital plane, of a punctual radiant energy source. During one orbital period the intensity of the day-night and summer-winter effects is determined by *sin θ'* and *cos θ'*: as one effect loses strength the other gains and vice-versa. To get a better visual graphic representation of the body moving around the energy source and the interplay between (1) and (2), we situate the spin axis on the orbital plane, but all qualitative conclusions are valid for the general case when $0 < \vartheta < \pi/2$. The day-night effect is strongly associated with the periodic recurrence between day and night that leads to the *xy* anisotropy. The summer-winter effect is associated with the length of the days and nights: long days, summer; long nights, winter and leads to the *z* anisotropy . We can identify two fundamental regions at the body surface: (1) day-night and summer-winter effects; (2) summer-winter effect.

Note that the area covered by these two regions change as the satellite moves along its trajectory. When the co-latitude of the energy source is zero or π we have only the type (2) region and the thermal re-emission force has only the $\mathbf{F}_z$ force component ($\mathbf{F}_{xy} = 0$), the summer-winter effect is maximum and the day-night effect vanishes. And, when $\theta' = \pi/2$ or $3\pi/2$ we have the opposite situation: only type (1) region and the thermal re-emission force has only the $\mathbf{F}_{xy}$ component ($\mathbf{F}_z = 0$), the day-night effect is maximum and the summer-winter effect vanishes. For intermediate angles we have both effects, with respective magnitudes ruled by the co-latitude of the energy source.

RADIAL AND ALONG-TRACK ACCELERATIONS

The radial and along-track accelerations can be obtained if we re-write **i** , **j** and **k** as a function of **r**, **s** and **w**. The relationship between these two reference systems centered at the satellite, (*x,y,z*) and (*r,s,w*), can be obtained by means of the Euler rotation matrices. We assume that the initial conditions (*t=0*) are: **i = s**; **j = -w** and **k = -r** (spin axis on the orbital plane). Rotation, translation, and spin axis movements will change the initial conditions. We can reproduce these changes if we apply three rotations to the (*x,y,z*) system:

$$R_3(-\omega t)\, R_1(\vartheta)\, R_2(nt)\,, \qquad (18)$$

where ω is the satellite's angular velocity of rotation, *n* is the satellite's mean motion, and the *z* axis inclination to the satellite's orbital plane. If the spin axis lies on the orbital plane, then $\vartheta = 0$ and we have:

$$\mathbf{i} = (\sin nt \cos \omega t)\mathbf{r} + (\cos nt \cos \omega t)\mathbf{s} + (\sin \omega t)\mathbf{w}, \qquad (19)$$

$$\mathbf{j} = (\sin nt \sin \omega t)\mathbf{r} + (\cos nt \sin \omega t)\mathbf{s} + (-\cos \omega t)\mathbf{w}, \qquad (20)$$

$$\mathbf{k} = (-\cos nt)\mathbf{r} + (\sin nt)\mathbf{s}, \qquad (21)$$

Now we will apply the relations above to the summer-winter and day-night effects separately. When the spin axis lies on the orbital plane $v_1 t = \omega t$, $v_2 t = nt$ and from Eq. (16) we have:

$$\mathbf{a}_{xy} = [2(1+\sin^2 nt)]^{-1} B_1 \sin(nt-\delta_2)[\cos(\omega t-\delta_1)\mathbf{i} + \sin(\omega t-\delta_1)\mathbf{j}]. \qquad (22)$$

Substituting Eqs. (19) and (20) into (22) leads to the radial and along-track accelerations, *R* and *S*. Averaging the radial and along-track accelerations over one rotation (<R> and<5>) we obtain:

$$\langle R \rangle \cong 0.15 C_2 \cos\delta_2 \cos\delta_1\,, \qquad (23)$$

$$\langle S \rangle \cong -0.20 C_1 \sin\delta_2 \cos\delta_1\,, \qquad (24)$$

$$\langle W \rangle = 0\,, \qquad (25)$$

where we assume that $C_1 = -B_1$ is constant along one integration period. And for the summer-winter effect we have:

$$\mathbf{a}_z = [2(1 + \sin^2 nt)]^{-1}\, B_2 \cos(nt - \delta_2)\, \mathbf{k}\,, \qquad (26)$$

Substituting Eq. (21) into (26) leads to the radial and along-track accelerations for the summer-winter effect. Averaging *R* and *S* over one rotation we obtain:

$$\langle R \rangle \cong 0.20 C_2 \cos\delta_2\,, \qquad (27)$$

$$\langle S \rangle \cong -0.15 C_2 \sin\delta_2\,, \qquad (28)$$

$$\langle W \rangle = 0\,, \qquad (29)$$

where we assume that for small eccentricities $C_2 = -B_2$ is constant along the integration period. For simplicity, in the following sections, we will refer to the mean radial and along-track accelerations only as radial and along-track accelerations.

APPLICATION: TEST-SATELLITE

The thermal re-emission effects can be better understand if we apply the relations obtained previously to a test-satellite. The main parameters of the test-satellite are based on the geo-dynamic satellite LAGEOS.

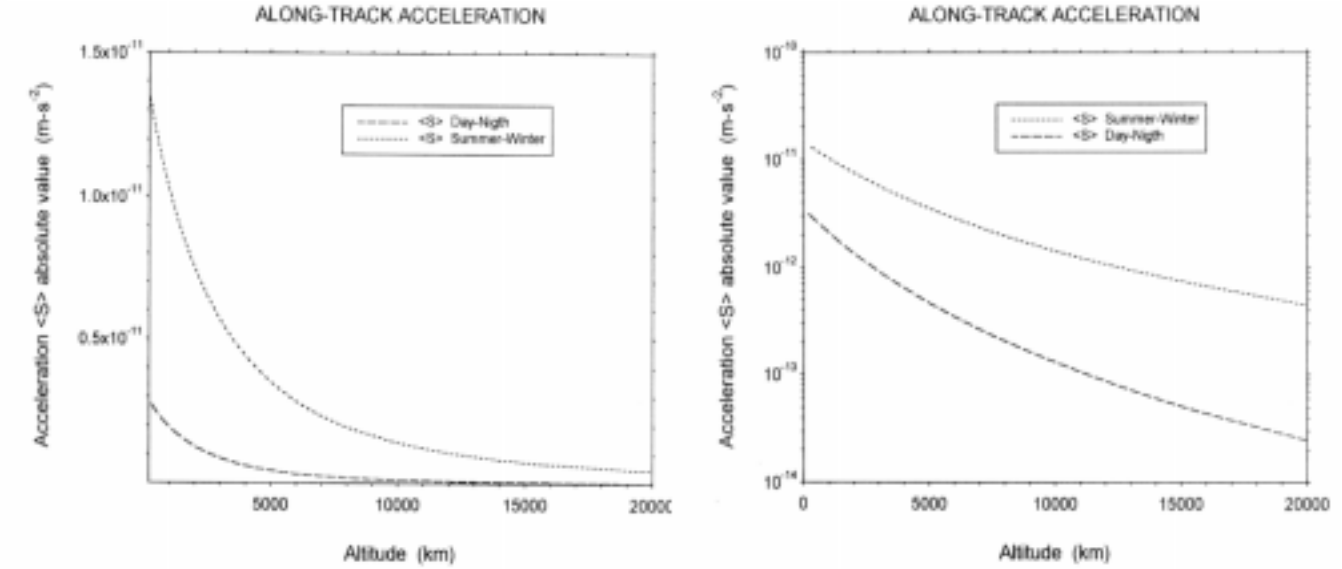

Figure 3 - The summer-winter and day-night averaged along-track accelerations absolute values for the test-satellite *versus* satellite's altitude.

Figura 3 *- Acelerações noite-dia e inverno-verão médias em valor absoluto para o satélite-teste versus a altitude do satélite.*

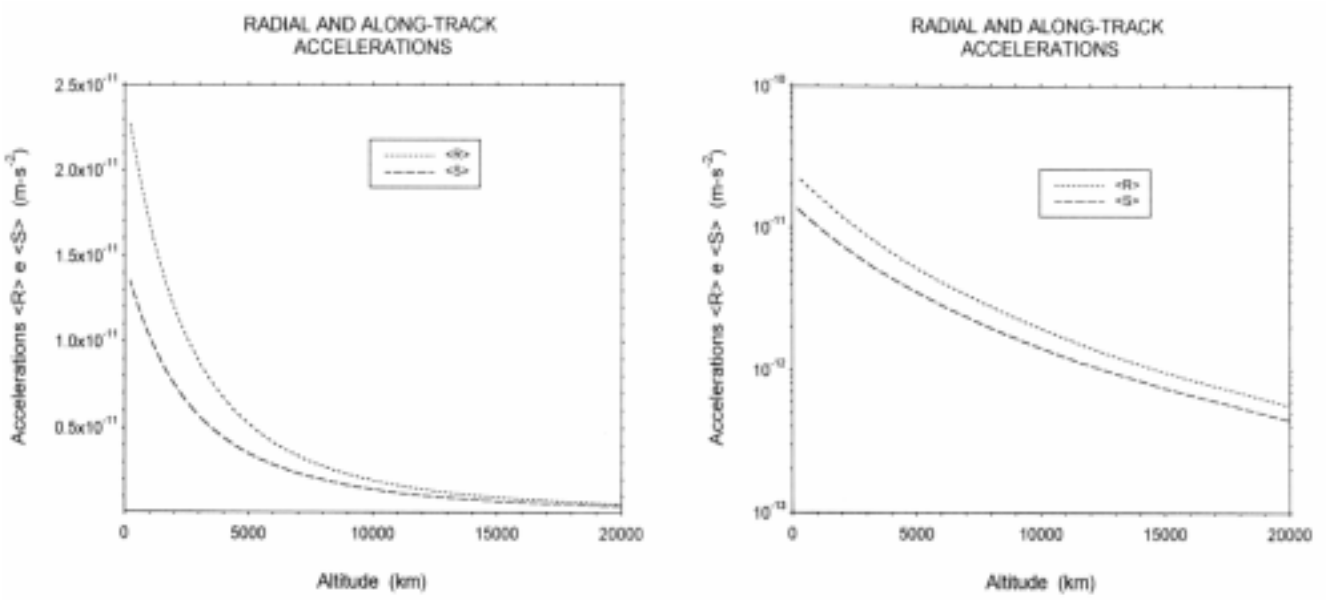

Figure 4 - The mean radial and along-track accelerations absolute values for the test-satellite *versus* satellite's altitude.

Figura 4 *- Acelerações radial e transversal médias em valor absoluto para o satélite-teste versus a altitude do satélite.*

The LAGEOS is a high-altitude satellite (6,000 *km*) moving around the Earth in an almost circular orbit (e = 0.004). The body of the satellite consist of two aluminum hemispheres bolted to a cylindrical beryllium copper core. About 42 % of its surface is studded with 422 fused silica laser retro-reflectors. "The prelaunch tests and theoretical estimations give temperature variations $\Delta T \approx 2$ to 3 K for the aluminum structure and $\Delta T \approx 20$ K between the two antipodal retro-reflectors. Hence, the photon thrust is primarily controlled by the retro-reflectors. The LAGEOS's orbit is modeled with high accuracy, however, after subtracting out most of the known forces acting on the satellite, such as the gravitational attraction of the Sun and moon, direct solar radiation pressure, etc., there is still a residual along-track acceleration that remains to be explained" (Rubincam, 1987; 1988; 1990; Rubincam et al., 1990).

There are, primarily, two important thermal energy sources providing thermal energy to the satellite:

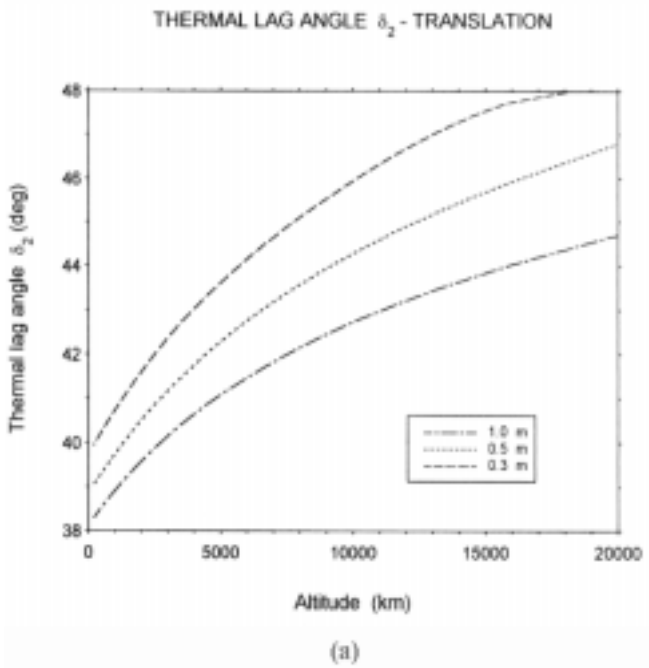

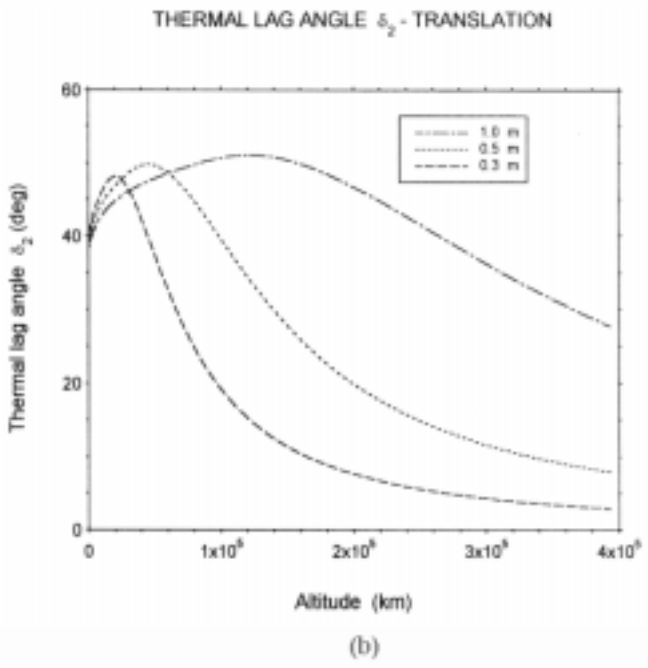

Figure 5a - The orbital thermal lag angle for the test-satellite *versus* altitude, for satellite's radii: 0.3, 0.5 and 1.0 m; with maximum altitude value 20,000 km.

Figura 5a *- Ângulo de atraso devido ao movimento orbital para o satélite-teste versus altitude, para os seguintes valores de raio de satélite: 0,3, 0,5 e 1,0 m; com altitude máxima igual à 20.000 km.*

Figure 5b - The orbital thermal lag angle for the test-satellite *versus* altitude, for satellite's radius: 0.3, 0.5 and 1.0 m; with maximum altitude value 400,000 km.

Figura 5b *- Ângulo de atraso devido ao movimento orbital para o satélite-teste versus altitude, para os seguintes valores de raio de satélite: 0,3, 0,5 e 1,0 m; com altitude máxima igual à 400.000 km*

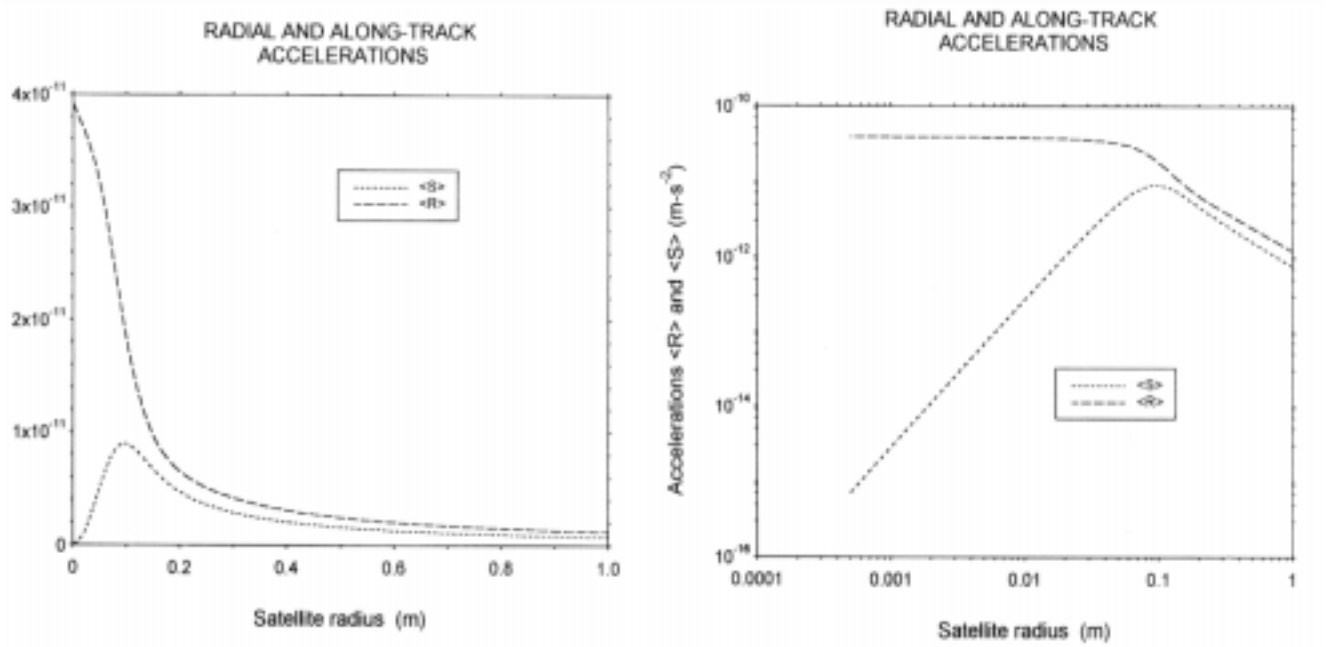

Figure 6 - The mean radial and along-track accelerations absolute values for the test-satellite *versus* the satellite's radius.

Figura 6 *- Acelerações radial e transversal médias, em valor absoluto, para o satélite-teste versus raio do satélite.*

the Sun (Rubincam et al., 1997) and the Earth. The radiance from the Sun is I_0 = 1,400 Wm^{-2} (1 *AU*) whereas the radiance from Earth is only I_0 = 62.55 Wm^{-2} (6,000 km). However, in the particular case presented here, where the satellite is orbiting the energy source, the contribution of the Earth for the along-track acceleration is more important. The satellite's orbital period of 1 year, with the Sun as the energy source, leads to a very small thermal lag angle and mean along-track component. However, for the real case, when the purpose of the work is to predict accurate satellite ephemeris, we should take into account both energy sources simultaneously.

Note that, for the next calculations and analyses, we assume that the test-satellite is homogeneous, spherical , with spin axis lying on the satellite orbital plane, and 100 % covered by fused silica retro-reflectors. Thus, we will take into account some fused silica retro-reflector constants, and the test-satellite main parameters as follows: semi-major axis, a = 1.227 x 10^7 m; orbital eccentricity, e = 0.004; mean motion, n = 4.64 x 10^{-4} s^{-1}; radius, R = 0.3 m; specific heat, Cp = 686 J kg^{-1} K^{-1}; emissivity, ε = 0.9; absorbity, a = 1.0; thermal conductivity, k = 1.34 W K^{-1} m^{-1}; density, ρ = 2200 kg m^{-3}. And we use also, the Earth infrared radiance, I_0 = 62.55 W m^{-2}; Earth radius, R_T = 6.371 x 10^6 m; Stefan-Boltzmann constant, s =5.67 x 10^{-8} W m^{-2} K^{-4}; and speed of light, c = 2.9979 x 10^8 m s^{-2}.

The radiance I_0 and the mean temperature T_0 are given by the following expressions:

$$I_0 = I_s\left(\frac{a_s}{a}\right)^2, \qquad (30)$$

$$T_0 = T_s\sqrt{\frac{a_s}{a}}, \qquad (31)$$

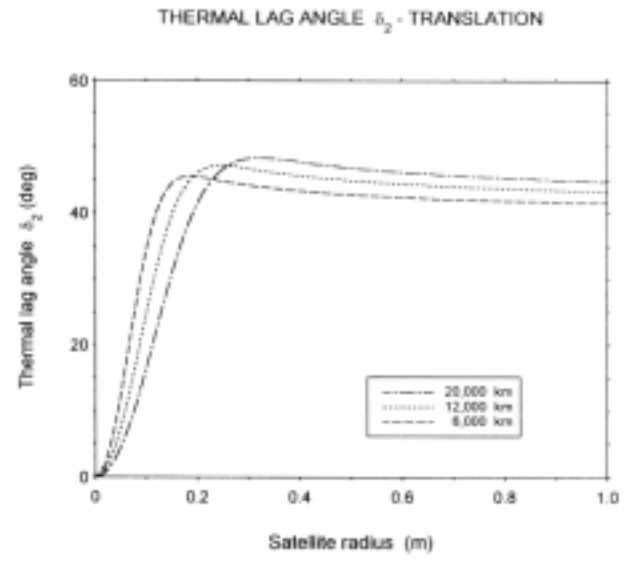

Figure 7 - The orbital thermal lag angle *versus* satellite's radius for the following altitudes: 6,000, 12,000 and 20,000 km.

Figura 7 *- Ângulo de atraso devido ao movimento orbital versus o raio do satélite para as seguintes altitudes: 6.000, 12.000 e 20.000 km.*

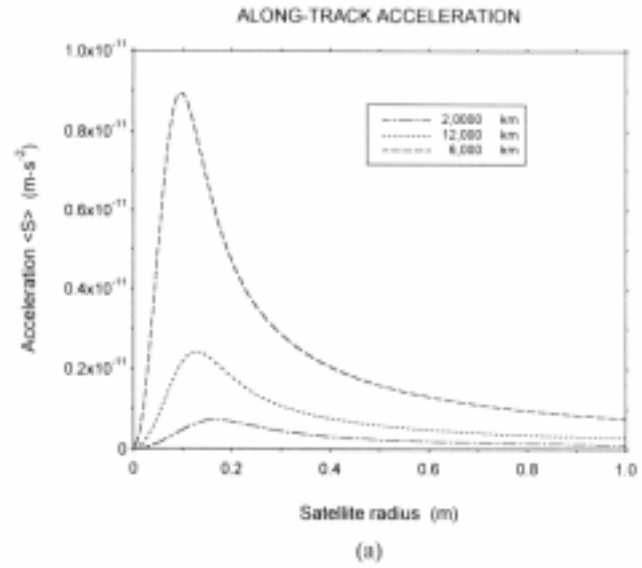

Figure 8a - The mean along-track acceleration *versus* satellite's radius for the following altitudes: 6,000, 12,000 and 20,000 km.

Figura 8a *- Aceleração transversal média versus o raio do satélite para as seguintes altitudes: 6.000, 12.000 e 20.000 km.*

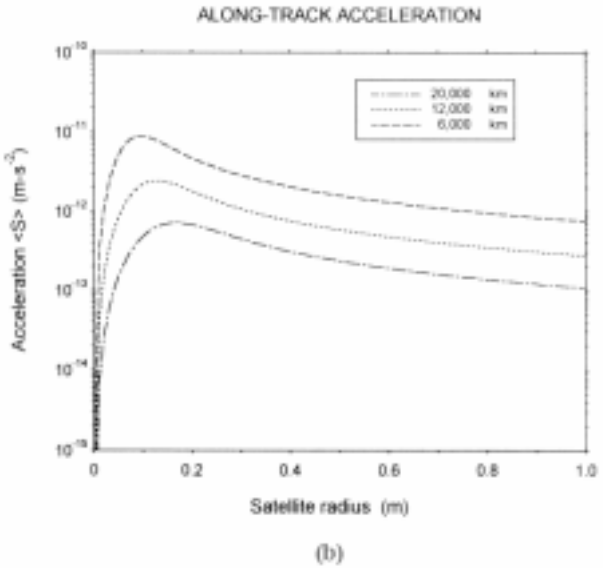

Figure 8b – Figure 8a in logarithmic scale .

Figura 8b *– Figura 8a em escala logarítmica.*

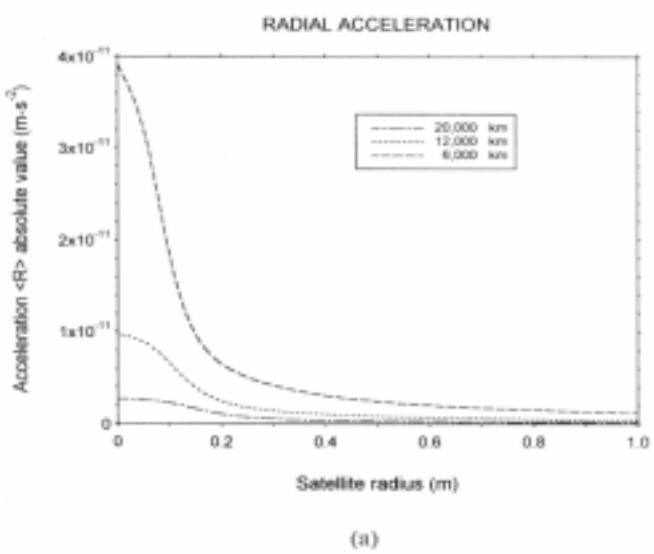

Figure 9a - The mean radial acceleration *versus* satellite's radius for the following altitudes: 6,000, 12,000 and 20,000 km.

Figura 9a *- Aceleração radial média versus raio do satélite para as seguintes altitudes: 6.000, 12.000 e 20.000 km.*

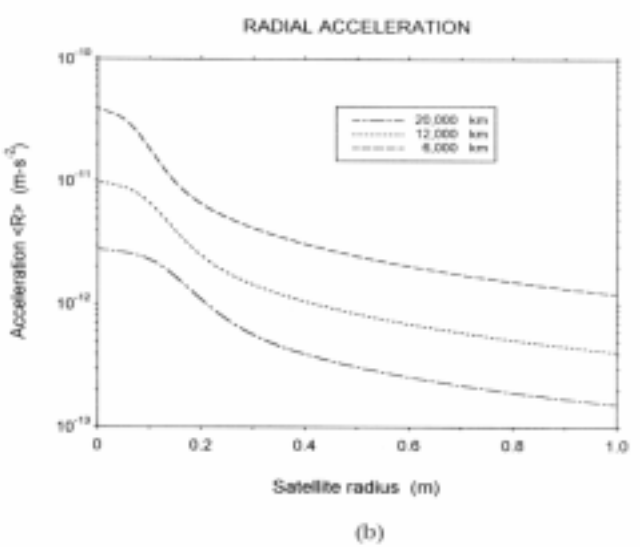

Figure 9b – Figure 9a in logarithmic scale.

Figura 9b *- Figura 9a em escala logarítmica.*

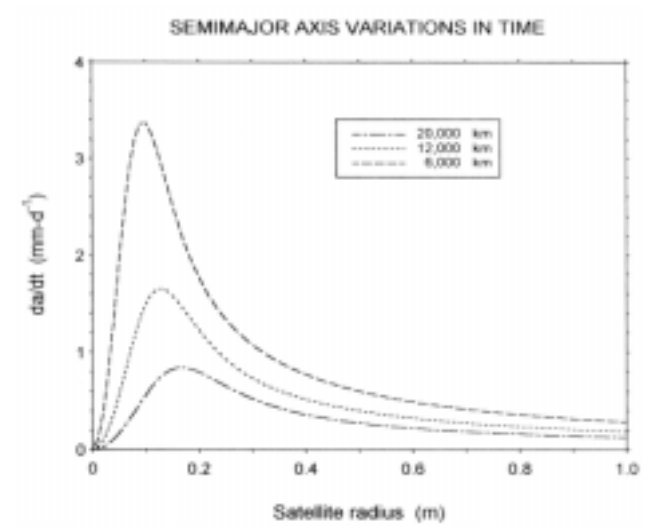

Figure 10 - The absolute value of the semi-major axis (or altitude) drift, due to the thermal re-emission effect, *versus* satellite's radius for the following altitudes: 6,000, 12,000 and 20,000 km.

Figura 10 *- Decaimento do semi-eixo maior orbital (ou altitude) em valor absoluto, devido ao efeito de re-emissão térmica, versus raio do satélite para as seguintes altitudes: 6.000, 12.000 e 20.000 km.*

where I_s = 62,55 W m^{-2} is the radiance from Earth at test-satellite altitude; T_s = 263 K is the test-satellite mean temperature; a_s = 1.227 x 10^7 m is the test-satellite semi-major axis; and a is the variable semi-major axis. The satellite's mean motion is given by:

$$n = \sqrt{(\mu / a^3)}\,, \qquad (32)$$

where μ is the Earth's universal gravitational parameter. When the rotational angular velocity is high the day-night effect can be neglected. In Fig. 3 we compare the summer-winter and day-night along-track absolute values when the satellite's spin period is 200 s. The summer-winter component is greater than the day-night one (nearly 6 % for 20,000 km) and this difference between components grows up for decreasing altitudes values.

For the test-satellite's altitude (6,000 km) the summer-winter along-track is:

$$\langle S \rangle = -2.85\times10^{-12}\, ms^{-2}\,, \qquad (33)$$

whereas, the day-night along-track is:

$$\langle S \rangle = -3.46\times10^{-13}\, ms^{-2}\,, \qquad (34)$$

that corresponds to nearly 12 % of the summer-winter along-track. However this difference gets smaller when the satellite's altitude increases (6 % for GPS altitudes: 20,000 km).

The day-night effect intensity depends crucially on the satellite's spin period. Since the LAGEOS spin period is increasing in time, from 1*s* just after launch to about 200 *s* now (*Rubincam et al.*, 1997), the day-night mean along-track contribution becomes more significant with time.

The total thermal force acting on the test-satellite, analyzed in this work, is due, mainly, to the summer-winter effect, and thus, the following procedures take into account only the thermal force component along the satellite's spin axis. Fig. 4 shows the radial and along-track accelerations absolute values as a function of the test-satellite's altitude.

The thermal lag angle δ_2 value is about 44 de-

grees ($\delta_1 \cong 45°$), and thus, the radial acceleration absolute value will be greater than the along-track one. With the Sun as the thermal radiation source, the thermal lag angle has a very small absolute value, and the difference between radial and along-track components grows in importance. The shape of the curves shown in Fig. 4 can be explained by the behavior of the thermal lag angle when the satellite's altitude varies (see Figs. 5a and 5b).

A similar analysis can be done if we plot the radial and along-track accelerations *versus* the radius of the satellite as shown in Fig. 6. The direction of the thermal force changes for different values of the satellite's radius. As the radius of the satellite gets smaller, the along-track acceleration loses strength for the radial component.

We can explain such behavior, also, by the analysis of the thermal lag angle, as we can see in the Fig. 7, that shows the thermal lag angle *versus* satellite's radius for altitudes 6,000, 12,000 and 20,000 km.

Figs. 8a and 8b show the along-track acceleration as a function of the satellite's radius for different altitude values. The curves present a peak for the following values of satellite's radii and altitudes: 0.10, 0.13 and 0.16 m, for 6,000, 12,000 and 20,000 km, respectively. Thus, the maximum of the along-track acceleration is displaced to the left when the satellite approaches the energy source.

Next, in Figs. 9a and 9b we repeat the analysis for the radial acceleration and obtain a similar behavior. The radial component also has a maximum associated to a very small satellite's radius, but in this case the maximum peak can be only partially visualized.

The secular variation in the semi-major axis can be obtained if we use the Gauss equation for non-gravitational perturbations:

$$\dot{a} = \frac{2}{n(1-e^2)^{1/2}}[R e \sin(f) + S(1+e\cos(f))], \quad (35)$$

where R and S are obtained by substituting Eq. (21) in Eq. (26):

$$R = -\frac{1}{2(1+\sin^2 f)} B_2 \cos(f - \delta_2)\cos(f), \quad (36)$$

$$S = \frac{1}{2(1+\sin^2 f)} B_2 \cos(f - \delta_2)\sin(f), \quad (37)$$

and $C_2 = C_0 / r^2$, with $B_0 = const$. For almost circular orbit, nt ≈ f, where f is the true anomaly.

Averaging Eq.(35) along one orbital period, we obtain:

$$\langle \dot{a} \rangle \cong 0.30 \frac{B_0 \sin\delta_2}{n}, \quad (38)$$

The effect is dissipative and the satellite's semi-major axis will decrease in time. The orbit decay is about:

$$\langle \dot{a} \rangle \cong 1.08\, mm\, d^{-1}. \quad (39)$$

Fig. 10 shows the semi-major axis decay for different satellite's radii values (from zero to 1.0 m). The more intense decay happens, as expected, for the lowest altitude (6,000 km). All the curves present a peak that associate the maximum semi-major axis decay to a satellite's radius. For our test-satellite (R = 0.3 m) the decay is about 1.08 millimeters per day, but this value will decrease to 0.25 millimeters per day for satellites with R = 1.0 m.

DISCUSSION

A satellite moving around the energy source will experience simultaneously both forces, summer-winter, $\mathbf{F}_z$, and day-night (generalized), $\mathbf{F}_{xy}$, but the intensity of these forces will change along the orbital period. A unified model should take into account the *sin θ'* and *cos θ'* terms for the Day-Night and Summer-Winter force components, respectively. These terms express the variations in the satellite's temperature distribution due to its movement around the energy source and allow to the simultaneous application of these two forces resulting in a unified Total Thermal force.

In order to simplify the analysis of the total thermal effect, we have neglected the day-night effect, in the previous section. To determine when one component of the thermal force can be neglected we should analyze the satellite's spin axis orientation and the satellite's main angular frequencies. In general, when the spin axis lies on the satellite's orbital plane ($\vartheta = 0$) the day-night effect can be neglected if $\omega >> n$ (high rotational frequency), but in the opposite situation, low rotational frequency, the day-night effect will play a more important rule than the summer-winter effect, and we can neglect this last one. Obviously that, to take into account both effects or only one depends on the accuracy you need. If the spin axis is perpendicular to the satellite's orbital plane ($\vartheta = \pi/2$) we can neglect the summer-winter effect without lost of accuracy, because in this case, the $\mathbf{F}_z$ component of the thermal force vanishes. For the remainder of the spin axis posi-

tions ($0 < \vartheta < \pi/2$), a simultaneous analysis of the spin axis inclination and the main satellite's angular frequencies will be necessary.

The total thermal force direction is controlled by the thermal lag angles δ_1 and δ_2. For our test-satellite, only d_2, the thermal lag angle due to the orbital motion, is important to determine the along-track and radial acceleration ratio. Since this angle increases when the satellite approach to the Earth, the along-track component gains intensity and the thermal effect becomes more important. However, for nearly 20,000 km (R_s = 0.3 m), δ_2 quickly decreases and, at this point, the thermal force orients all on the radial direction.

Note that the *z* component of the total thermal re-emission acceleration is always dissipative, whereas the *xy* component can be either dissipative or anti dissipative depending on the sense of the rotation. For small bodies with high angular rotational velocity the summer-winter effect dominates and the total thermal effect is dissipative. For the opposite situation when the day-night dominates the total thermal effect can be either dissipative or anti dissipative. The dissipative attribute of the thermal forces will lead to the semi-major axis and altitude decrease shown in the Fig. (10) that result in the shrinking of the satellite's orbit.

Finally, one important characteristic of the thermal re-emission force should be remarked: the well defined and localized maximum points for the thermal re-emission along-track component that strongly increases at some critical values of altitude and satellite's radii, and "selects" the satellite that will be more affected by the thermal force. According to this results satellites to be launched in the future should take into account the problem dimension-altitude, in order to avoid the maximum points of the thermal forces, and consequently the maximum orbit decay.

The forecoming work encompasses results for satellite's arbitrary spin axis orientation, and considers the simultaneous use of both effects.

REFERENCES

AFONSO, G. B. & FORYTA, D.W. – 1989 - An anisothermical emission model for small bodies, in Orbital Dynamics of Natural and Artificial Objects (R. Vieira-Martins, D. Lazarro & W. Sessin Eds.), pp. 73-83. Observatorio Nacional, Rio de Janeiro.

AFONSO, G. B., BARLIER, F., BERGER, C. & MIGNARD, F. – 1980 - Effet du freinage atmosphérique et de la traînée électrique sur la trajectoire du satellite LAGEOS. *C.R.* Acad. Sci. Paris, Ser. B**, 290**: 445-448.

AFONSO, G. B., BARLIER, F., BERGER, C., MIGNARD, F. & WALCH, J.J. – 1985 - Reasessment of the charge and neutral drag of LAGEOS and its geophysical implications. J. Geophys. Res., **90**: 9381-9398.

AFONSO, G. B., BARLIER, F., CARPINO, M., FARINELLA, P., MIGNARD, F., MILANI, A. & NOBILI, A.M. – 1989 - Orbital effects of LAGEOS seasons and eclipses. Ann. Geophys., **7**: 501-514.

BERTOTTI, B. & IESS, L. – 1991 - The rotation of LAGEOS. J. Geophys. Res., **96**: 2341-2440.

DUHA, J. – 1996 - Modelagem e aplicações do efeito Inverno-Verão, Tese de Mestrado, Departamento de Ciências Exatas, Universidade Federal do Paraná, Brasil.

FARINELLA P., VOKROUHLIKY D. & BARLIER F. – 1996 - The rotation of LAGEOS and its long-term semimajor axis decay; a self-consistent solution. J. Geophys. Res., **101**: 17861-17872.

MIGNARD, F., AFONSO, G.B., BARLIER, F., CARPINO, M., FARINELLA, P., MILANI, A. & NOBILI, A.M. – 1990 - LAGEOS: ten years of quest for the non-gravitational forces. Adv. Space Res., **10**: 221-227.

RUBINCAM, D.P. – 1987 - LAGEOS orbit decay due to infrared radiation from Earth. J. Geophys. Res., **92**: 1287-1294.

RUBINCAM, D.P. – 1988 - Yarkovsky thermal drag on LAGEOS. J. Geophys. Res., **93**: 13805-13810.

RUBINCAM DP. – 1990 - Drag on the LAGEOS satellite. J. Geophys. Res., **95**: 4881-4886.

RUBINCAM, D.P., CURRIE, D.G. & ROBBINS, J.W. – 1997 - LAGEOS I once-per-revolution force due to solar heating. J. Geophys. Res., **102**: 585-590.

Manuscript submitted April 4, 1999
Revised version accepted October 25, 1999

THERMAL FORCE EFFECTS ON SATELLITES

Todos os objetos no espaço são regularmente aquecidos por fontes de energia térmica. A investigação de efeitos térmicos associados a esse aquecimento é capaz de explicar alguns aspectos inesperados da evolução orbital de naves espaciais viajando através do espaço além de, proporcionar a otimização da modelagem orbital de satélites artificias em órbita ao redor da Terra.

O mecanismo que gera a força térmica que atua em satélites artificiais é muito simples: a radiação proveniente de uma fonte de radiação térmica (Sol, Terra, etc...) incide na superfície do satélite, aquecendo com maior eficiência o lado do satélite voltado para a fonte de radiação, do que o lado oposto (lado escuro). Como conseqüência, a superfície do satélite apresenta uma distribuição de temperaturas assimétrica. O lado quente re-emite fótons mais energéticos e portanto, perde mais momento do que o lado frio. Esta

anisotropia leva à um momento linear resultante diferente de zero e, consequentemente, à uma força resultante que irá atuar no satélite. A quantidade de radiação recebida por um elemento de superfície na unidade de tempo varia de acordo com as coordenadas da fonte de energia, que são controladas pela orientação do eixo de rotação do satélite, e por seu movimento de rotação e de translação. Há duas assimetrias fundamentais na superfície do satélite que regulam a distribuição de temperaturas: uma ao longo do eixo de rotação (conhecida como efeito inverno-verão) e outra no plano equatorial (efeito noite-dia), no sistema de referência do satélite.

As forças de origem térmica tem sido apontadas como a principal causa do decaimento orbital residual, observado em satélites artificiais de grande altitude. Estas forças estão associadas à acelerações na ordem do picometro (10^{-12}ms^{-2}). Neste trabalho, propomos um modelo térmico que apresenta o efeito térmico total como a soma dos efeitos Inverno-Verão e Noite-Dia "generalizado". Mostramos que um modelo unificado deve levar em consideração o termo *sin θ'* para a componente noite-dia da força térmica (longitudinal) e o termo *cos θ'* (onde *θ'* é a colatitude da fonte de energia térmica) para a componente inverno-verão da força térmica (latitudinal). Estes termos estão associados à variações de temperatura na superfície do satélite devidas ao seu movimento ao redor da fonte de energia térmica e permitem a aplicação simultânea dessas duas forças, resultando em uma força térmica total unificada que possui duas componentes: a força Inverno-Verão, na direção do eixo de rotação do satélite (*z*), e a força Noite-Dia generalizada, no plano equatorial do satélite (*xy*).

A orientação do eixo de rotação do satélite em relação a fonte emissora de radiação é muito importante, pois determina a intensidade dos efeitos inverno-verão e noite-dia. Durante um período orbital a intensidade das foças $\mathbf{F}_{xy}$ (noite-dia) e $\mathbf{F}_{z}$ (inverno-verão) sofre mudanças cíclicas determinadas por *sen θ'* e *cos θ'*, respectivamente; enquanto um efeito perde força o outro ganha e vice-versa, e isto se repete quatro vezes para uma revolução completa.

De uma forma geral, a direção da força térmica total é controlada por dois ângulos de atraso térmico associados ao movimento orbital e ao movimento de rotação do satélite. Além disso, a altitude e as dimensões do satélite são variáveis capazes de alterar a direção, módulo e sentido dessa força térmica.

A componente inverno-verão da aceleração é responsável por um efeito dissipativo, enquanto que, a componente noite-dia pode resultar em ambos os efeitos, dissipativo ou antidissipativo, dependendo do sentido do movimento de rotação do satélite em relação ao movimento orbital. Para objetos com alta velocidade angular de rotação, de uma forma geral, o efeito inverno-verão é dominante e o efeito térmico total é dissipativo. Para a situação oposta, quando o efeito noite-dia é dominante, o efeito térmico total pode ser dissipativo ou antidissipativo. A qualidade dissipativa das forças térmicas irá levar ao decréscimo do semi-eixo maior resultando em um decaimento da órbita do satélite.

Neste trabalho, aplicamos as forças de re-emissão térmica à um satélite-teste (parâmetros baseados em dados do satélite LAGEOS) e obtemos a perturbação resultante em termos da aceleração transversal média, para o efeito noite-dia, $\langle S \rangle = -3{,}46 \times 10^{-13}$ ms^{-2}, e para o efeito inverno-verão, $\langle S \rangle = -2{,}85 \times 10^{-12}$ ms^{-2}, que leva à um decaimento orbital residual de aproximadamente 1,08 mmd^{-1}.

Além disso, analisamos o comportamento das acelerações radial e transversal médias, e do ângulo de atraso em função da altitude do satélite, e obtemos uma "lei de seleção" que associa o efeito térmico máximo ao raio e a altitude do satélite.

NOTE ABOUT THE AUTHORS

Jânia Duha

Has a degree in Physics from the Universidade Federal do Paraná (UFPR), Curitiba, Brazil, where she obtained, in April 1996, her M.Sc. in Sciences with the thesis "Modeling and applications of the Summer-Winter effect". She presented the Unified Thermal Model for the summer-winter and day-night effects, and pointed out the existence of a Selection Law associated with the total thermal re-emission force and its components. Since then, she has been worked extensively with the application of the thermal re-emission forces on Asteroids and on Artificial Satellites. Currently, she is at the UFPR's Department of Geomatics, where she is working on her Ph.D. thesis on thermal force effects on artificial satellites.

Germano Bruno Afonso

Is a full professor in the Department of Physics at the Universidade Federal do Paraná (UFPR), Curitiba, Brazil, where he has been teaching since 1973. He has a degree in Physics and a MSc. in Geodesy from the Universidade Federal do Paraná and a Dr. Sc. in Astronomy from the Université Pierre et Marie Curie, Paris, France. Dr. Afonso has worked extensively with Non-Gravitational Forces Modelling Effects on Artificial Satellites and Asteroid Fragments Orbits. His research interests are related also with Dynamical Evolution of the Earth-Moon System and with Brazilian Archaeoastronomy.